IOP Conference Series: Materials Science and Engineering

PAPER • OPEN ACCESS

Grain size assessment using EBSD on heterogeneous additively manufactured microstructures

To cite this article: J del Gaudio *et al* 2024 *IOP Conf. Ser.: Mater. Sci. Eng.* **1310** 012028

View the article online for updates and enhancements.

IOP Conf. Series: Materials Science and Engineering **1310** (2024) 012028 doi:10.1088/1757-899X/1310/1/012028

Grain size assessment using EBSD on heterogeneous additively manufactured microstructures

J del Gaudio[1*], J Donoghue[1], P J Withers[1], A Garner[1,2], K Mingard[3], M Gee[3] and A Gholinia[1]

[1] Henry Royce Institute, Department of Materials, University of Manchester, Manchester, M13 9PL, United Kingdom

[2] Jacobs, Warrington, United Kingdom

[3] National Physical Laboratory, Teddington, United Kingdom

*E-mail: jacopo.delgaudio@manchester.ac.uk

Abstract. Grain microstructures are important for a whole range of materials properties. With the widespread use of additive manufacturing (AM), current standards for grain boundary evaluation, such as ASTM E2627-13, may not be fit for purpose due to their microstructural complexity. They are notoriously anisotropic across a range of length scales due to the non-equilibrium nature of the solidification process and the tracking of the heat source. In this work we examine the grain microstructure of a nickel superalloy produced by laser powder bed AM by electron back scatter diffraction. We find that the guidelines provided by the ASTM E2627-13 are not suitable for such heterogeneous and anisotropic materials and some modified guidelines are provided on the field of view and EBSD step size that should be used to characterise such materials.

1. Introduction

Grain size measurement is widely undertaken in industry and research and is a fundamental property that can significantly affect the overall material behaviour. The influence of grain size on the deformation and failure of polycrystalline metal is well documented, and for many models that have been developed to predict the performance of the materials, such as the Hall-Petch equation [1] for predicting yield strength.

The measurement procedure for grain size by electron backscatter diffraction (EBSD) is standardized by the ASTM E2627-13(2019) [2], which is an extension of the ASTM E112 (2021) [3], that is based on stereological principles [4]. It states that in order to perform an EBSD grain size measurement in compliance with the standard some requirements need to be met:

- No more than 10% of the points should be unindexed.
- The grains should be defined with grain boundary (GB) misorientation above 5°.
- Multiple maps can be used with minimum of 50 grains in each map until at least 500 grains have been measured.
- The average grain should contain about 500 pixels in the EBSD map.
- All grains must contain more than 100 pixels.

Following these guidelines the average area of the grains is calculated by $\bar{A} = \frac{1}{n}\sum_i^n A_i$ where A_i is the area of the grain i. The standard deviation is calculated on the average area of the grain $\bar{A}$. Finally, the ASTM grain size number "G" is calculated by using the formula $G = (-3.3223 \cdot \log \bar{A}) - 2.995\bar{A}$, where $\bar{A}$ is in mm². This procedure is based on stereological principles that assume the "independent uniform and random" (IUR) [4] selection of the grains on each map and the Gaussian distribution of the resulting grain size population.

Additive manufactured (AM) materials are built-up layer by layer in the "build direction" (BD) by melting and rapidly solidifying (cooling rate of 10^4-10^6 K/s [5]) the raw material in the form of powder or wire. The resulting microstructure is highly anisotropic and it exhibits a substantial divergence from a Gaussian distribution arrangement [6] due to the complex thermal history as well as a very wide range of grain sizes.

The aims of this work are to examine the extent to which the ASTM standard is suitable for the measurement of the grain size in AM materials, what parameters can be used to define the microstructure and to measure the grain size, and what EBSD conditions should be used in order obtain reliable and representative analyses.

2. Experimental details

2.1 Materials

The exemplar material studied is AM Hastelloy X produced on an EOS M400-4 laser powder bed system with a sinusoidal grid raster, using a powder with a nominal composition: Ni 47 wt.%, Cr 22 wt.%, Fe 18 wt.%, Mo 9 wt.%, Co 1.5 wt.%, W 0.6 wt.%, C 0.1 wt.%, Mn 1 wt.%, Si 1 wt.%, B 0.008 wt.%, Nb 0.5 wt.%, Al 0.5 wt.%, Ti 0.15 wt.%.

2.2 EBSD measurement and post-processing

The AM block was cut parallel to the BD. The samples were polished using standard mechanical procedure. The EBSD maps were acquired on a Zeiss Auriga 60 with an Oxford Instruments Symmetry 2 detector, at electron beam power of 30 kV and current of 10 nA. A small area map of 766 µm x 480 µm with a total area of 0.37 mm^2 was acquired at processing 1076 patterns/s with step size of 0.5 µm. A larger area map of 4293 µm x 1306 µm with a total area of 8.76 mm^2 (A_0) was acquired with the detector processing 2311 patterns/s and a step size of 1.25 µm. Each map was postprocessed using AZtecCrystal 2.2. The clean-up procedure consisted of "Auto Clean-Up", "Remove Wild Spikes", "Zero Solution Removal" with the level of "5-Five Neighbourhood" and 10 iterations on the small area map and the same procedure but with level of the zero solution removal at "4 -Four Neighbourhood" 10 iterations on the large area map. A total of 221813 pixels for the small area map (7%) and 505311 pixels for the large area map (9%) have been replaced, (i.e. within the ASTM guidelines).

3. Results and discussion

3.1 Setting the grain boundary criteria

The first step is to define what represents a grain boundary (GB). Figure 1 shows the highly anisotropic structure, both in terms of grain shape, with small equiaxed grains at melt pool boundaries and large elongated grains along the BD direction and a variety of differently shaped small grains, from equiaxed to elongated. The 5 and 10° GB criteria are highlighted by the white and black lines respectively. From this it is clear that the white lines represent sub-grain boundaries (21% of the total) and the black predominantly high angle GBs (79%). Clearly for this AM system the 5° misorientation proposed by ASTM is not appropriate, indeed it could be argued whether 10° is sufficient misorientation to correctly segment the grains. Throughout this paper 10° is used as the GB criteria.

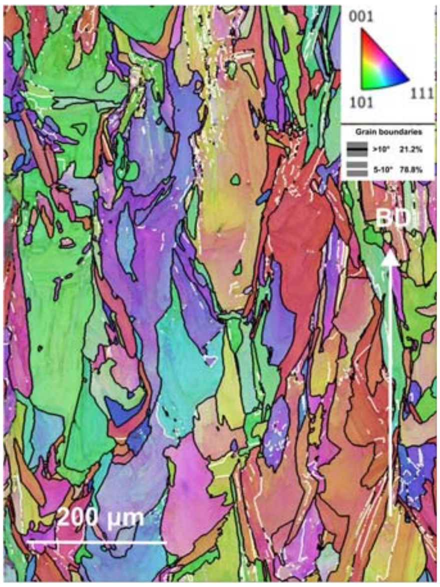

Figure 1. Small area EBSD map of Hastelloy X AM, in IPF-Z colours, step size 0.5 µm, 1533x480 pixels with the BD vertical. The 5° criteria is illustrated by the white lines, the 10° misorientation by the black lines.

3.2 Area required for grain size analysis

Collecting large area maps is time consuming. In this section we examine the distribution of grain sizes to examine whether it conforms to the Gaussian distribution and look at the dimensions necessary that should be used or exceeded to define a statistically representative grain size. We divided the large area (A_0) map in figure 2 into six progressively smaller subset sizes ($A_0/2$, $A_0/4$, $A_0/8$, $A_0/16$, $A_0/32$, $A_0/64$). This is done by progressively halving perpendicular to the BD (e.g. dashed white lines) or parallel to the BD (the white solid lines). In each subset size, 8 patches of the microstructure are taken at different locations. The area and equivalent circle diameter of the grains are measured, including only the grains that are wholly within the patch. Over the whole area (A_0) a total of 4522 grains have been detected with an average equivalent circle diameter of 36.7 µm and area weighted equivalent circle diameter of 94.5 µm.

The average equivalent circle diameters measured from the six subsets parallel to the BD and the six subsets perpendicular to the BD are compared in figure 3. For the subsets parallel to the BD the results show similar mean values for the four larger fields of view with the standard

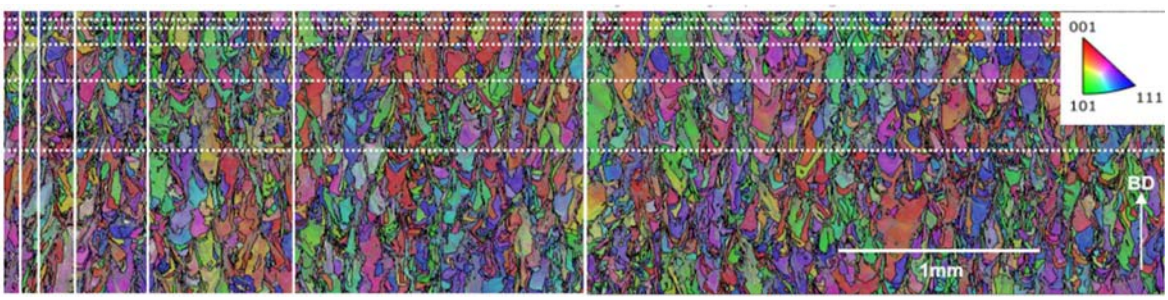

Figure 2. Large area EBSD map (A_0) in IPF-Z colours with the strategy to divide into subsets parallel to the BD in solid white lines and perpendicular to BD in dotted lines.

deviation increasing as the field of view decreases. This might suggest that a subset area ¼ or even ⅛ as wide as A_0 might suffice. By contrast for the subset areas perpendicular to the BD the results only begin to plateau for the $A_0/2$ subset area and this suggests that an area equal to the full height of the image in figure 2 is required. This result is of course related to the elongated shape of the larger grains and consequently the likelihood of cutting very large grains which, due to their orientation, are unlikely to be fully included in the field of view of the subset perpendicular to the BD. In both cases the average tends to smaller grain sizes as the sampled area becomes smaller because few larger grains lie within the subset area, because grains at the boarder are excluded. Therefore, similar number of grains need to be covered in either direction by matching the aspect ratio of the larger grains and the EBSD map.

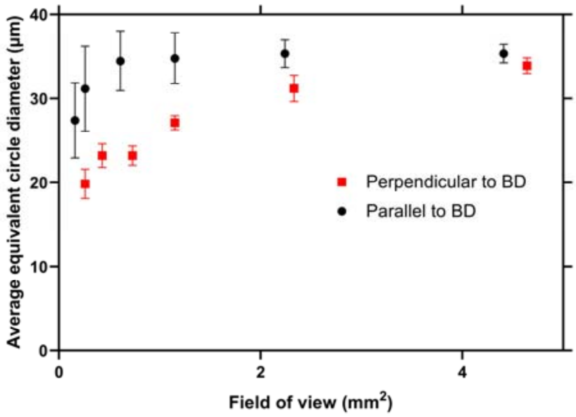

Figure 3. Measurement of the average grain equivalent circle diameter for the differently sized subsets from the large area map (A0/2, A0/4, A0/8, A0/16, Ao/32, A0/64) and 8 patches for each subset.

3.3 Step size required for grain size analysis

As well as considering the size of the patch sampled it is important to consider the sampling step size. Using a small step size over a large area is very cost and time inefficient while sampling at a coarse step size will exclude the smaller grains. In order to examine this the grain size (equivalent circle diameter) population was assessed for the largest subset ($A_o/2$) from the large area map using a step size of 1.25 µm and 2.5 µm by sub-sampling by 2x2. These populations are shown in figure 4(a) as histogram with bin width calculated with the Freedman-Diaconis rule [7] of 3.1µm. The resulting distribution is evidently highly non-Gaussian (contravening the ASTM requirement) and shows that over 40% of grains lie within the first three bins of the distribution for the 1.25 µm map. The distribution of the 2.5 µm map shows essentially the same distribution but with a different cut off due to the threshold on the minimum number of pixels (100) defining the grain in the grain detection procedure which determines the smallest recordable diameter for a grain. As a result the number fractions change significantly because >40 % of the grains recorded for the smaller step size are unrecorded such that the grain average increases from 39 µm for 1.25µm step size to 50µm at 2.5µm. Such a skewed population distribution means that the finer the step size the smaller the average measured grain size. However, as one would expect, it is clear from the grain area weighted population distribution in figure 4(b) that these smaller grains exert a smaller and smaller influence on the area weighted grain size. As a result the area weighted average grain size is much less dependent on the step size being 96 and 97 for the 1.25 and 2.5µm step sizes respectively.

The implications of this wide and highly skewed grain size distribution on the average grain size is shown in figure 5 as a function of the different sampling patch areas. For the reasons noted above, the change in step size introduces a significant shift towards a larger average grain size as

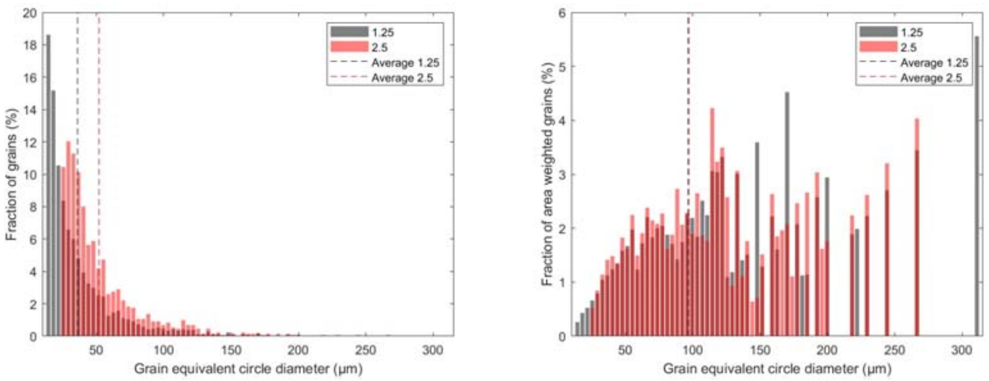

(a) **(b)**

Figure 4. (a) Distribution of the grain equivalent circle diameter for the largest subset $(A_0/2)$ parallel to the BD with step size 1.25 µm (grey) and 2.5 µm (red). (b) Distribution of the grain area weighted diameter over the grain equivalent circle diameter for the largest subset parallel to the BD with step size 1.25 µm (grey) and 2.5 µm (red).

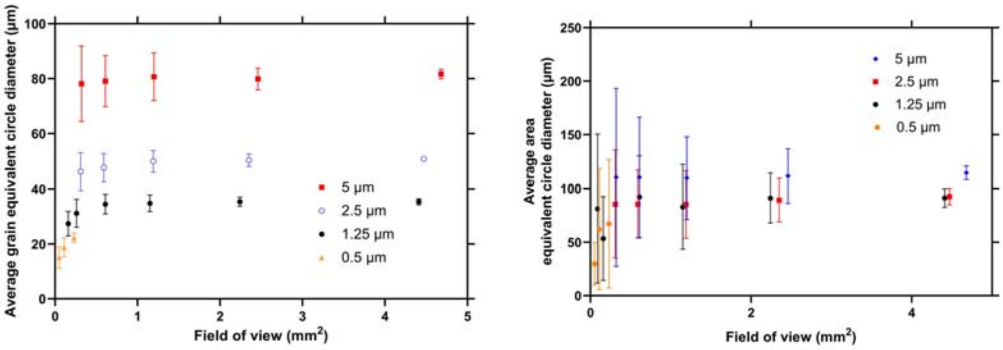

(a) **(b)**

Figure 5. Measurement of the a) average equivalent circle diameter and b) average area equivalent circle diameter for the differently sized subsets with 8 patches from each subset, which are sampled from the large area map as a function of the EBSD step size.

the step size is increased. By contrast the area average grain size is much less affected by the step size although the scatter increases as the size of the sampling subset is decreased.

4. Conclusions

In this paper we have looked at the suitability of the ASTM standard for grain size measurement for a typical AM microstructure. The grain structure is highly anisotropic and the grain size varies greatly from very small grains and very large columnar grains. The following conclusions are made:

1. 10° misorientation is a more appropriate grain boundary criterion than 5° because of the highly developed sub grain structure.
2. The grain size distribution in this AM microstructure is not Gaussian as required in ASTM standard, therefore it is not possible to follow the ASTM standard.
3. The average equivalent circle diameter reduces with reduction in step size, which is due to the possibility to capture finer grains at finer step sizes.
4. Because of the large tail of the fraction of very small grains, the average equivalent circle diameter is affected by the cut off or threshold used for allowable minimum grain diameter. However the average equivalent circle diameter is less affected by the threshold used for minimum grain diameter when considering the area weighted grain fraction.
5. The area or field of view required to achieve good grain size statistics in an EBSD map needs to have similar number of grains perpendicular and parallel to BD. Therefore the aspect ratio of an EBSD map for these types of AM microstructures will the aspect ratio of the grains.
6. The average weighted area fraction is less dependent on step size, which is a more robust method to capture grain size in such microstructures.

In an ideal world it would be preferable to measure the grain size in 3D using plasma dual beam or laser tribeam microscopy [8]. Future work is underway to determine the minimum block size required for characterisation of AM 3D complex grain structure. This work can provide guidelines on the dimensions of the sampled area and the in-plane step size that should be employed.

Acknowledgements

The authors are grateful for the resources provided by the Electron Microscopy Centre funded by the Henry Royce Institute (EP/X527257/1) for providing the microscopy capability. JdG is grateful for the sample and the funding provided by the National Physical laboratory and Jacobs.

References

[1] Hall E O 1951 The deformation and ageing of mild steel: III discussion of results *Proc. Phys. Soc. B* **64** 747

[2] Standard practice for determining average grain size using electron backscatter diffraction (EBSD) in fully recrystallized polycrystalline materials 2019 **ASTM E2627-13**

[3] Standard test methods for determining average grain size 2021 **ASTM E112-13**

[4] Wojnar L 2020 Stereology *Encyclopedia of Mathematical Geosciences* Springer international publishing ed B S Daya Sagar et al Cham: Springer International Publishing 1–12

[5] Mostafaei A, Ghiaasiaan R, Ho I, Strayer S, Chang K, Shamsaei N, Shao S, Paul S, Yeh A, Tin S and To A C 2023 Additive manufacturing of nickel-based superalloys: A state-of-the-art review on process-structure-defect-property relationship *Prog. Mater. Sci.* **136** 101108

[6] Zhang LC, Liu Y, Li S and Hao Y 2017 Additive Manufacturing of Titanium Alloys by Electron Beam Melting: A Review *Adv. Eng. Mater.* **20** 1700842

[7] Freedman D and Diaconis P 1981 On the histogram as a density estimator: L2 theory *Probab Theory Relat Fields* **57** 453

[8] Gholinia A, Donoghue J, Garner A, Curd M, Lawson M J, Winiarski B, Geurts R, Withers P J and Burnett T L 2024 Exploration of fs-laser ablation parameter space for 2D/3D imaging of soft and hard materials by tri-beam microscopy *Ultramicroscopy* **257** 113903